

Cellular Uptake of Arginine-Rich Peptides: Roles for Macropinocytosis and Actin Rearrangement

Ikuhiko Nakase,¹ Miki Niwa,¹ Toshihide Takeuchi,¹ Kazuhiro Sonomura,¹ Noriko Kawabata,¹ Yukihiko Koike,¹ Masanori Takehashi,¹ Seigo Tanaka,¹ Kunihiro Ueda,¹ Jeremy C. Simpson,³ Arwyn T. Jones,^{4,*} Yukio Sugiura,¹ and Shiroh Futaki^{1,2,†}

¹Institute for Chemical Research, Kyoto University, Uji, Kyoto 611-0011, Japan

²PRESTO, JST, Kawaguchi, Saitama 332-0012, Japan

³Department of Cell Biology and Biophysics, EMBL–Heidelberg, 69117 Heidelberg, Germany

⁴Welsh School of Pharmacy, Cardiff University, Cardiff CF10 3XF, Wales, UK

*To whom correspondence and reprint requests should be addressed at the Welsh School of Pharmacy, Cardiff University, Redwood Building, King Edward the VII Avenue, Cardiff CF10 3XF, UK. Fax: +44 2920 874536. E-mail: jonesat@cardiff.ac.uk.

†To whom correspondence and reprint requests should be addressed at the Institute for Chemical Research, Kyoto University, Uji, Kyoto 611-0011, Japan. Fax: +81 774 32 3038. E-mail: futaki@scl.kyoto-u.ac.jp.

The use of membrane-permeable peptides as carrier vectors for the intracellular delivery of various proteins and macromolecules for modifying cellular function is well documented. Arginine-rich peptides, including those derived from human immunodeficiency virus 1 Tat protein, are among the representative classes of these vectors. The internalization mechanism of these vector peptides and their protein conjugates was previously regarded as separate from endocytosis, but more recent reevaluations have concluded that endocytosis is involved in their internalization. In this report, we show that the uptake of octa-arginine (R8) peptide by HeLa cells was significantly suppressed by the macropinocytosis inhibitor ethylisopropylamiloride (EIPA) and the F-actin polymerization inhibitor cytochalasin D, suggesting a role for macropinocytosis in the uptake of the peptide. In agreement with this we observed that treatment of the cells with R8 peptide induced significant rearrangement of the actin cytoskeleton. The internalization efficiency and contribution of macropinocytosis were also observed to have a dependency on the chain length of the oligoarginine peptides. Uptake of penetratin, another representative peptide carrier, was less sensitive to EIPA and penetratin did not have such distinct effects on actin localization. The above observations suggest that penetratin and R8 peptides have distinct internalization mechanisms.

Key Words: HIV-1 Tat, arginine-rich peptides, internalization, protein delivery, protein transduction, cell-permeable peptide, penetratin, macropinocytosis, actin rearrangement

INTRODUCTION

The use of membrane-permeable carrier peptides as cellular delivery vectors has recently received widespread attention [1–5]. Intracellular delivery of various molecules, including oligonucleotides, peptide nucleic acids, and even liposomes (diameter 200 nm), has been reported using this approach. One of the most representative carrier peptides is an arginine-rich peptide derived from human immunodeficiency virus type 1 Tat protein [Tat (48–60)] [2,6] and considerable efforts have been focused on the elucidation of its internalization mecha-

nism. The internalization of these peptides was originally described as being largely unaffected by low-temperature incubation or treatment with typical endocytosis inhibitors, and therefore pathways independent of endocytosis were hypothesized [6]. However, recent reports shed doubt on these results and a revision of the proposed mechanisms of internalization was recently published [7]. One of the reasons for this misunderstanding is attributed to the effects of fixation on the microscopic observation of the internalized peptides. Fixation was shown to cause significant artifacts on the cellular localization of peptides. Additionally, strong adsorption of the

peptides to the cell surface is also suspected to lead to misinterpretation of fluorescence microscopy images.

Until now, various carrier peptides were reported to have an ability to co-internalize exogenous molecules into cells [1–5,8–13]. However, it is not known whether the internalization mechanism of carrier peptides into cells is in any way dependent on their associated payloads. It is also unclear whether the physicochemical properties of the cargo molecules have a significant effect on the mode of internalization.

We previously reported that, depending on the number of arginine residues in the molecules, oligoarginine peptides showed differential manners of internalization and cellular localization [11,12]: R4 (tetramer of arginine) did not show significant internalization, R8 (octamer) showed efficient internalization and nuclear localization very similar to that of Tat (48–60), whereas R16 (hexadecamer) showed less efficient internalization compared to Tat (48–60) without showing significant nuclear localization. However, these observations were obtained using fixed cells, and therefore for the reasons described above, a reexamination of the possible routes of internalization of these molecules is necessary before their potential as delivery vectors is fully understood.

Macropinocytosis is a lipid raft-mediated and clathrin- or caveolae-independent endocytic process [14,15], with the sizes of the macropinosomes being often greater than 1 μm . If macropinosomes are leaky as has been suggested [16], it is possible to reason a number of phenomena for the internalization mechanisms of Tat peptide via this route. For example, it was reported that liposomes containing surface Tat peptides entered the cells as intact structures without fusion with the plasma membrane [17]. The size of the liposomes was 200 nm and therefore somewhat larger than a classical clathrin-coated pit (~120 nm) or caveolae invagination (~60 nm). We previously confirmed that the plasma membranes of cells remained intact after internalization of arginine peptides using a lactate dehydrogenase release assay [12]. These results can be explained if the peptides were able to permeate through endocytic membranes into cytosol.

Using a Tat-Cre fusion protein, Dowdy and co-workers recently suggested that raft-mediated macropinocytosis plays a crucial role in Tat-mediated cellular uptake of proteins [18]. They also showed that cellular uptake of the Tat-fusion protein was inhibited by treatment with inhibitors such as amiloride, a Na^+/H^+ exchange protein inhibitor, which has been documented to inhibit macropinocytosis.

Understanding the internalization mechanism of carrier peptides is fundamental to their use as delivery vectors. In view of the recent data regarding uptake of the Tat-fusion protein by macropinocytosis, we examined whether arginine-rich carrier peptides and penetratin

were also internalized into cells via this mechanism. We investigated the mechanism of cell entry of selected oligoarginine peptides and demonstrated that they have different mechanisms of uptake and that macropinocytosis may be a contributing process. In support of this, addition of arginine peptides resulted in pronounced actin reorganization, a function reported to accompany macropinocytosis [15,16].

RESULTS

Fluorescence Microscopy of Unfixed HeLa Cells Treated with R8 Peptide

We first confirmed that fixation of the cells significantly affected the cellular distribution of arginine-rich peptides. Octa-arginine (R8) was used as a representative of arginine-rich peptides since they showed internalization characteristics similar to those of the Tat peptide [11,12]. Fig. 1A shows representative confocal images of HeLa cells treated with Texas red-labeled R8 peptide (10 μM) at 37°C for 1 h. The nuclei were visualized using SYTO 11, which freely permeates the membranes of living cells. As reported by others [7,19–21], the peptide was localized to punctate perinuclear structures but there was no evidence of nuclear labeling. This is in contrast to the fixed cells (Fig. 1B), in which the peptide is diffusely localized throughout the cytosol and also to a certain extent in the nucleus. This confirms that there is a considerable difference in the apparent cellular localization of the R8 peptide between fixed cells and living cells. Compared with 37°C, cellular uptake of both peptides, as judged by FACS analysis, was significantly reduced at 4°C by 39 and 31%, for R8 and DR8 (octamer of D-arginine) peptides, respectively (Fig. 1C). In these experiments we washed the cells five times with PBS and treated them with trypsin prior to assessing the amount of the internalized peptide by FACS. These observations suggested that a fraction of the peptides were internalized in a temperature-dependent manner possibly via endocytosis. Assuming that the surface-adsorbed R8, and not DR8, peptides were susceptible to tryptic degradation, the difference in the fluorescence intensity from the R8- and DR8-treated cells would correspond to the amount of surface-adsorbed peptides, which we estimated to be less than 10%.

When we incubated the cells with R8 peptide in the presence of transferrin, we observed very little colocalization of both labels in punctate structures under the given condition (see Fig. S1A in Supplementary Material). The uniquely R8-positive structures were often considerably larger than the transferrin-positive vesicles, suggesting that they may have arisen from an endocytic route different from the well-characterized clathrin-dependent one that is known to be utilized by the transferrin receptor. Alternatively, it is also possible that both labels were internalized via the same endocytic

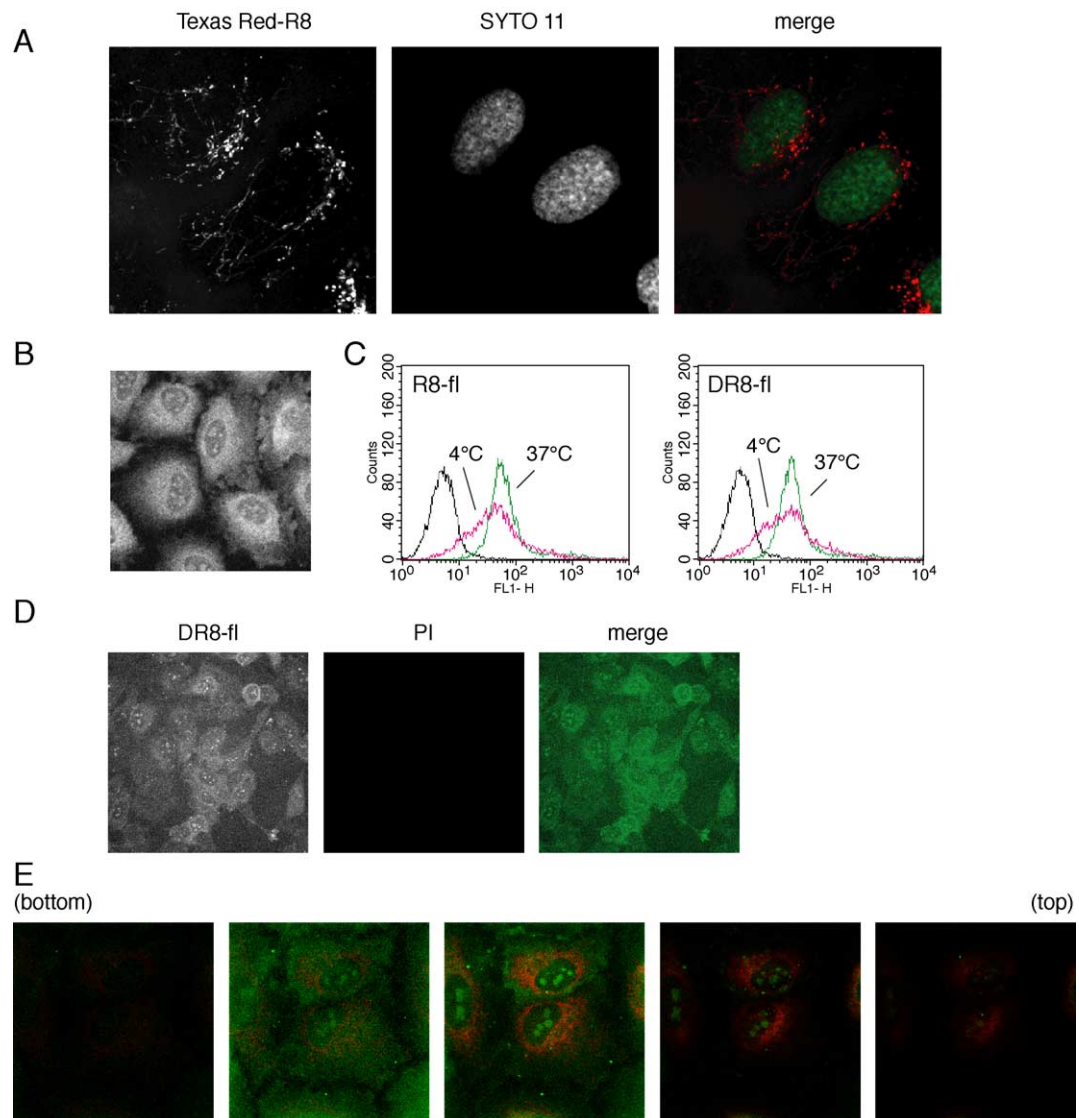


FIG. 1. Internalization of R8 peptide into HeLa cells. (A) Confocal microscopy analysis of living HeLa cells incubated at 37°C for 1 h with the Texas red-labeled R8 peptide (10 μ M) (red). Nuclei were stained with SYTO (No. 11) (5 μ M) (green). (B) Effect of fixation on cellular localization. Cells were treated with Texas red-labeled R8 as stated above and fixed with acetone:methanol (1:1) for 1 min on ice prior to imaging. (C) Quantification of the cellular uptake of R8-fl or DR8-fl at 37 and 4°C. Cells were incubated with peptides (10 μ M) for 1 h at 37 and 4°C prior to trypsinization and FACS analysis. Green, 37°C; red, 4°C; black, control cells. (D) Incubation of cells with DR8-fl peptide at 4°C. Prior to addition of the peptide, the cells were kept in the refrigerator (4°C) for 1 h. They were then incubated with peptide (10 μ M) (green) in the presence of propidium iodide (PI) (5 μ M) (red) for 1 h, washed with cold PBS, and observed by confocal microscopy in ice-cold, fresh culture medium. (E) Cross section along the z axis of the cells treated with DR8-fl peptide at 4°C for 1 h. The cells were incubated with the DR8 peptide as above except that MitoTracker (250 nM) (red) was used to outline mitochondria rather than PI, which was added to the cells 30 min before the washout of the peptides. Each picture represents a 1.2- μ m interval from the bottom (left) to the top (right).

route but were then differentially sorted into separate endocytic compartments.

When we incubated cells with DR8-fl peptide for 1 h at 4°C, a very different pattern of labeling was observed compared to the cells incubated at 37°C (Fig. 1D). There was significant background staining suggesting some of the label was being adsorbed to the glass surface. The cellular labeling was significantly higher than back-

ground but was diffusely distributed throughout the cell, including the nucleus. We did not observe any of the characteristic punctate labeling that was so apparent at 37°C. Fig. 1D also shows that the plasma membrane was intact since it did not allow access of propidium iodide (PI) to label the nucleus. To determine whether the label was “intracellular” rather than on the glass or cell surface we performed confocal z-axis sectioning of cells incu-

bated at 4°C with DR8-fl and observed that the vast majority of the label was confined to the lower section of the cells (Fig. 1E). This was in contrast to mitochondria labeling with MitoTracker, which was more evenly distributed through the cell slices. DR8-fl staining of the nucleus and especially the nucleolus was, however, apparent in three of the five cell sections, suggesting that a fraction of the label was able to translocate to this compartment.

Internalization of R8 Peptide by Macropinocytosis

We next examined the possibility that macropinocytosis contributes to the cellular uptake of R8 peptide. To do this we incubated cells in the presence of the macropinocytosis inhibitor 5-(*N*-ethyl-*N*-isopropyl)amirolide (EIPA) [15,16]. Cells were pretreated with EIPA (100 μ M) for 30 min and then incubated with fresh medium containing R8 peptide (10 μ M) in the presence of EIPA (100 μ M). After 1 h, we washed the cells and observed them directly by confocal microscopy. The cellular uptake of R8 peptide was significantly lower in the presence of EIPA (Fig. 2A), and FACS analysis showed a 31% reduction in R8 peptide uptake compared with untreated cells (Fig. 2B). EIPA had only a minor effect on transferrin uptake.

Rearrangement of the actin cytoskeleton during macropinocytosis is well documented [15,16]—macropinosomes are formed from cell surface membrane ruffles folding back on the plasma membrane, with actin playing a crucial role. To confirm the possibility of the involvement of actin rearrangement or membrane ruffling in arginine peptide mediated macropinocytosis, we examined the morphology of F-actin in cells treated with R8 peptide. We treated the cells with R8 peptide (10 μ M) for 30 min and then stained them with phalloidin-tetramethylrhodamine isothiocyanate (TRITC) after fixation (Fig. 2E). To avoid the effects of serum-containing growth factors that may induce membrane ruffling, we incubated the cells with the peptide in the absence of serum. We observed significant rearrangement of F-actin in the cells treated with the R8 peptide (Fig. 2E) and the effects were visible from as early as 5 min after peptide loading (data not shown). Epidermal growth factor (EGF) is known to cause membrane ruffling [16] and we observed a similar rearrangement of F-actin in cells treated with 10 nM EGF (Fig. 2E). Interestingly, we observed a 20% increase in R8 peptide uptake when the cells were co-incubated in the presence of EGF (Fig. 2C), whereas EGF gave no significant effect on the cellular uptake of transferrin (data not shown).

We further confirmed the contribution of F-actin to the internalization of R8 peptide by treating the cells with cytochalasin D (CytD), which is known to induce depolymerization of F-actin (Fig. 2F). Following incubation with CytD (5 μ M), cellular R8 peptide was predominantly localized to cellular boundaries and very little

punctate staining was observed. Phase-contrast observation also demonstrated that CytD treatment induced significant morphological changes in the cells. To confirm that this was not mediated by cell death, we washed the cells with fresh medium and incubated them in fresh medium in the absence of CytD for 3 h (Fig. 2G). At the end of the 3-h wash period, cellular morphology returned to normal, suggesting that the effects of CytD were reversible and that the inhibition of cellular uptake of R8 peptide by CytD treatment was not due to cell death but to the effects of this agent on F-actin polymerization.

Microtubules are also required for endocytic processes and we next determined whether R8 uptake in cells was microtubule dependent. For this we incubated cells with R8 peptide, in the presence or absence of the microtubule depolymerizing agent nocodazole, and analyzed R8 uptake by fluorescence microscopy (Fig. S1B in Supplementary Material) and FACS (Fig. 2D). Both methods revealed a reduction in R8 peptide uptake in the presence of this drug and FACS analysis showed an average decrease of 29% compared with untreated cells.

We next determined whether any of the internalized R8 peptide was recycled to the cell surface and released into the medium. For this we treated the cells with either rhodamine-labeled transferrin (which is known to recycle [14]) or rhodamine-labeled R8 (10 μ M) for 30 min prior to washing them with fresh medium and incubating them in the absence of the protein or peptide for a further 30 min. Confocal microscopy confirmed that the transferrin signal had disappeared by the end of the chase period but a significant amount of the peptide remained in the cells (Fig. S1C in Supplementary Material).

We then analyzed R8 peptide dynamics in cells by live cell imaging (see Videos 1 and 2 in Supplementary Material). We incubated the cells with rhodamine-labeled R8 peptide (3.5 μ M) for 45 min, washed them with fresh medium, and then imaged them using a Perkin-Elmer spinning disc confocal microscope equipped with a CCD camera. We observed a significant number of labeled motile endosome-like structures in these cells and a number of these structures also appeared to fuse with each other. The directed transport of some of these structures suggested that they were moving along cytoskeletal structures. In addition, a number of larger non-motile structures were also visible.

Reexamination of the Mechanism of the Cellular Uptake of R4, R8, and R16 Peptides

We previously reported differences in internalization mechanisms between oligoarginine (R_n , $n = 4-16$) peptides using fixed cells [11]. In these cells, little internalization was observed for the R4 peptide in contrast to much higher internalization and nuclear localization of

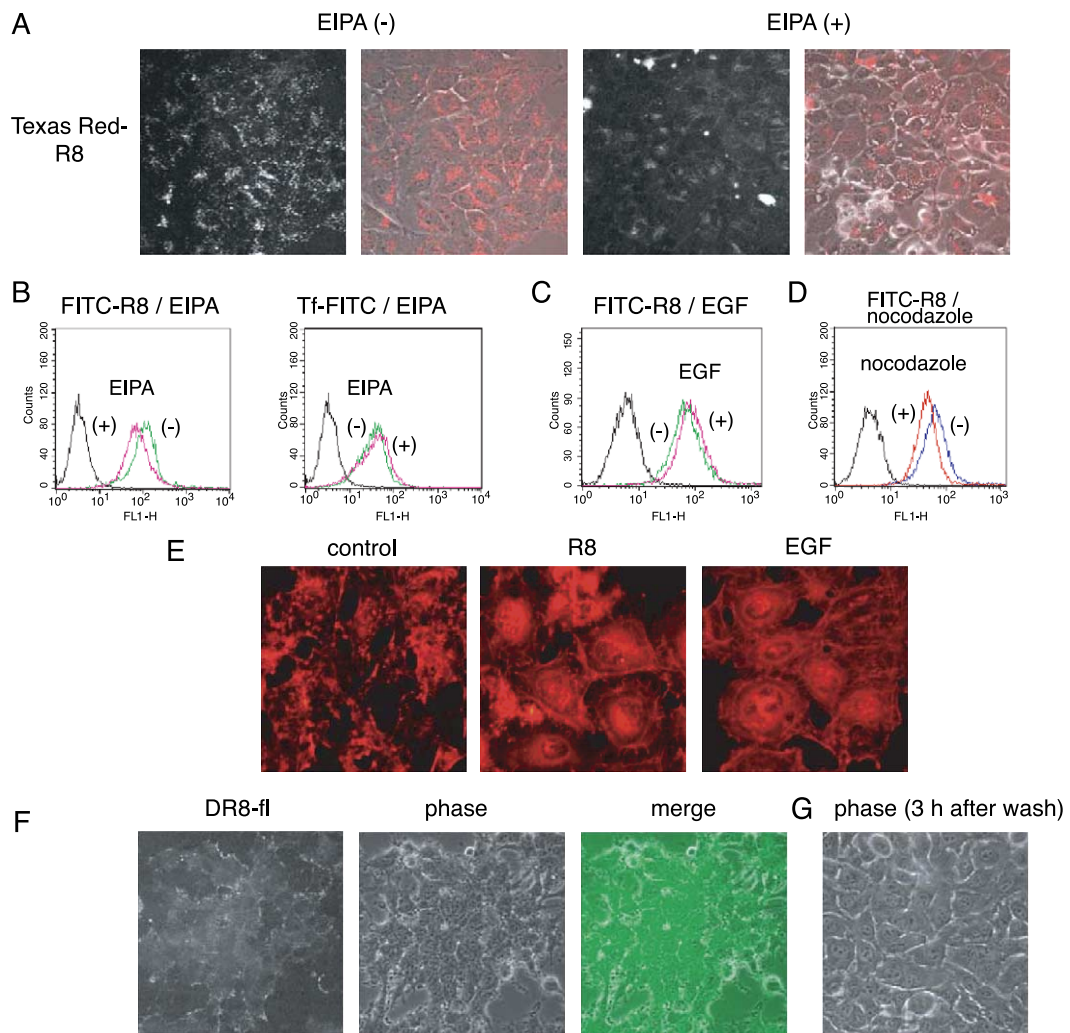


FIG. 2. Contribution of macropinocytosis to the cellular uptake of R8 peptide. (A) Cellular uptake of Texas red-R8 by the cells treated in the presence of the macropinocytosis inhibitor 5-(*N*-ethyl-*N*-isopropyl)amirolide (EIPA). HeLa cells were initially pretreated with EIPA (100 μ M) at 37°C for 30 min. The medium was replaced with fresh medium containing Texas red-R8 (10 μ M) and EIPA (100 μ M). The cells were incubated for 1 h, washed with PBS, and observed by confocal microscopy. For comparison, the cells were incubated with the peptide (10 μ M) for 1 h in the absence of EIPA. Shown are merges of phase contrast and fluorescence images of Texas red-R8-treated cells. (B) FACS analysis of cellular uptake of FITC-R8 (10 μ M) and transferrin (Tf)-FITC (25 μ g/ml) in the presence (red line) and absence (green line) of EIPA (100 μ M). Cells were treated as above using FITC-R8 instead of Texas red-R8. Black line, control cells. (C) Increase in cellular uptake of FITC-R8 in the presence of EGF. Prior to FACS analysis, HeLa cells were incubated in α -MEM containing 1% BSA in the absence of serum for 24 h and treated with the peptide (10 μ M) in the presence (red line) and absence (green line) of EGF (10 nM) for 15 min in α -MEM. Black line, control cells. (D) Inhibition of cellular uptake of FITC-R8 by nocodazole. Cells were pretreated with nocodazole (10 μ M) at 37°C for 15 min and incubated with FITC-R8 (10 μ M) in the presence (red line) or absence (blue line) of nocodazole (10 μ M) for 30 min. Black line, control cells. (E) Actin rearrangement in HeLa cells induced by R8 peptide and EGF. Cells were treated with R8 peptide (10 μ M) or EGF (10 nM) as described under Materials and Methods and observed by fluorescence microscopy. (F) Inhibition of cellular uptake of the DR8-fl peptide by cytochalasin D (CytD). Cells were pretreated with CytD (5 μ M) at 37°C for 15 min and then incubated with DR8-fl (10 μ M) (green) in the presence of CytD (5 μ M) for 30 min. (G) Almost complete recovery of the cellular structure was attained by washing out of peptide and CytD with PBS followed by incubation for 3 h in fresh medium. (For interpretation of the references to colour in this figure legend, the reader is referred to the web version of this article.)

R6 and R8 peptides. Further increases in arginine residues, however, led to a decrease in internalization efficiency and nuclear localization. We now know that fixation can cause significant effects on intracellular quantities and distribution of these peptides. Therefore we reexamined R4 and R16 uptake and distribution in living cells and compared the results with those for the R8 peptide (Fig. 3).

We observed little internalization of the R4 peptide (green in Fig. 3A compared with mitochondria in red) in the living cells, although we did see significant uptake of R16 peptide. We also observed punctate patterns of labeling for this peptide, suggesting uptake via an endocytic pathway. Quantification of cell-associated peptides by FACS revealed that the degree of cellular

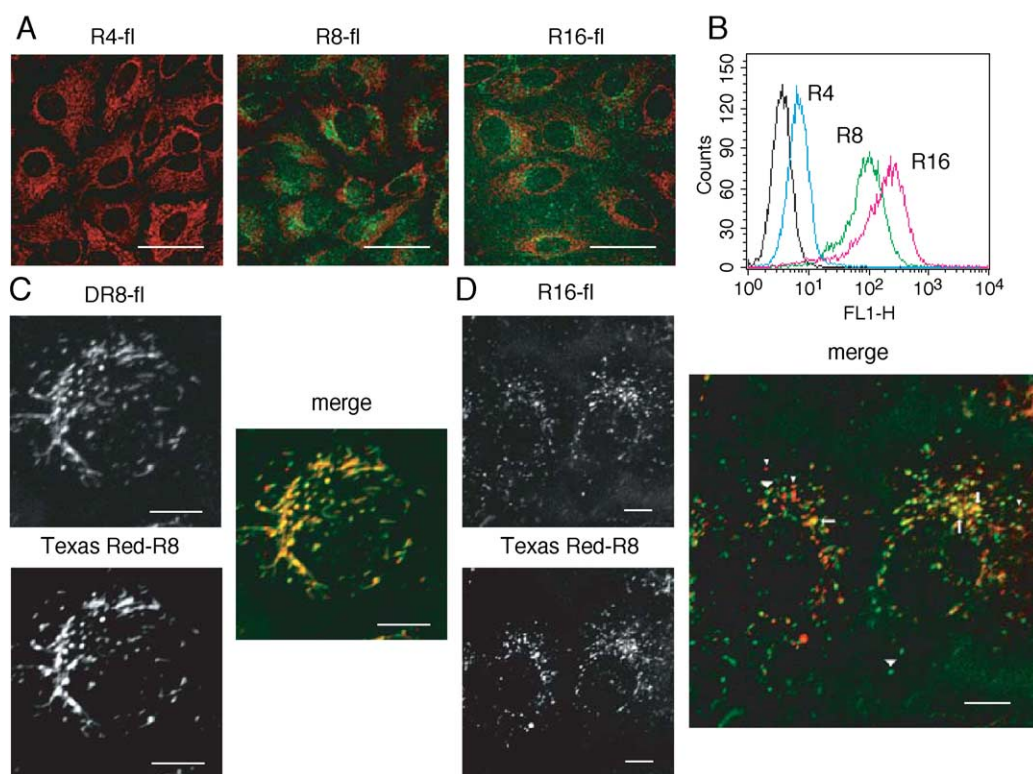


FIG. 3. Analysis of the cellular uptake R4, R8, and R16 peptides. (A) Confocal microscopy of cells treated with oligoarginine peptides. The cells were treated with 10 μ M R4-, R8-, and R16-fl peptides (green), for 1 h. MitoTracker (250 nM) (red) was added 30 min before peptide washout. Scale bar, 50 μ m. (B) FACS analysis of the cells treated with oligoarginine peptides. Cells were treated with 10 μ M FITC-R4 (blue line), -R8 (green line), and -R16 (red line) peptides for 1 h and subjected to FACS analysis. Black line, control cells. (C) Colocalization of DR8-fl (green) and Texas red-R8 peptides (red) in HeLa cells. Cells were incubated with DR8-fl and Texas red-R8 for 1 h in medium. Image of the perinuclear area is shown. Scale bar, 10 μ m. (D) Cellular localization of R8 and R16 peptides. Cells were incubated with Texas red-R8 (red) and R16-fl (green) (10 μ M each) as above and visualized by confocal microscopy. Colocalization of R8 and R16 is shown by arrows, R8 vesicles by small arrowheads, and R16 vesicles by large arrowheads. Scale bar, 10 μ m.

uptake of the R16 peptide was in fact higher than that of the R8 peptide (Fig. 3B).

To obtain further information on the cellular uptake of the R16 peptide, we examined whether the R8 and R16 peptides colocalized to the same vesicular compartments. Initially we determined whether fluorescein or Texas red labeling or utilization of the D (DR8) and L forms of the peptides had a critical effect on cellular localization using the fluorescein-labeled DR8 and Texas red-labeled R8 peptides (Fig. 3C). Fluorescein-labeled DR8 and Texas red-labeled R8 colocalized extensively in these cells, suggesting that fluorescent labeling with the above dyes or the chirality of the R8 peptides was not crucial to the cellular localization of these peptides. When we incubated the cells with fluorescein-labeled R16 in the presence of Texas red-labeled R8 peptide, however, considerable numbers of structures labeled by the respective peptides did not colocalize (Fig. 3D), suggesting that there might be differences in uptake mechanisms and/or intracellular processing.

We next determined whether R16 uptake was sensitive to EIPA and whether, like R8, the R16 peptide induces actin rearrangements. Treating cells with 100 μ M EIPA had a greater inhibitory effect on R16 uptake (Fig. 4A) compared to our earlier results with the R8 peptide (Fig. 2A). R8 internalization was reduced by 31% by EIPA; however, similar FACS analysis demonstrated a 54% inhibition in R16 uptake (Fig. 4B). We also observed significant reorganization of F-actin in cells treated with 10 μ M R16 peptide (Fig. 4C). There were, however, significantly greater morphological effects on cells treated with R16 compared to those treated with R8. Phase-contrast observation of the cells treated with 50 μ M R16 peptide revealed that the cells had rounded and shrunk (data not shown), and this was reflected in the F-actin structures in the cells treated with 50 μ M R16 peptide (Fig. 4C). The morphological difference could therefore be due to the higher cytotoxicity of the R16 peptide compared to the R8 peptide, which was subsequently confirmed by the MTT [3-(4,5-dimethylthiazol-2-yl)-2,5-diphenyl-2H-tetrazolium bromide] assay (see below).

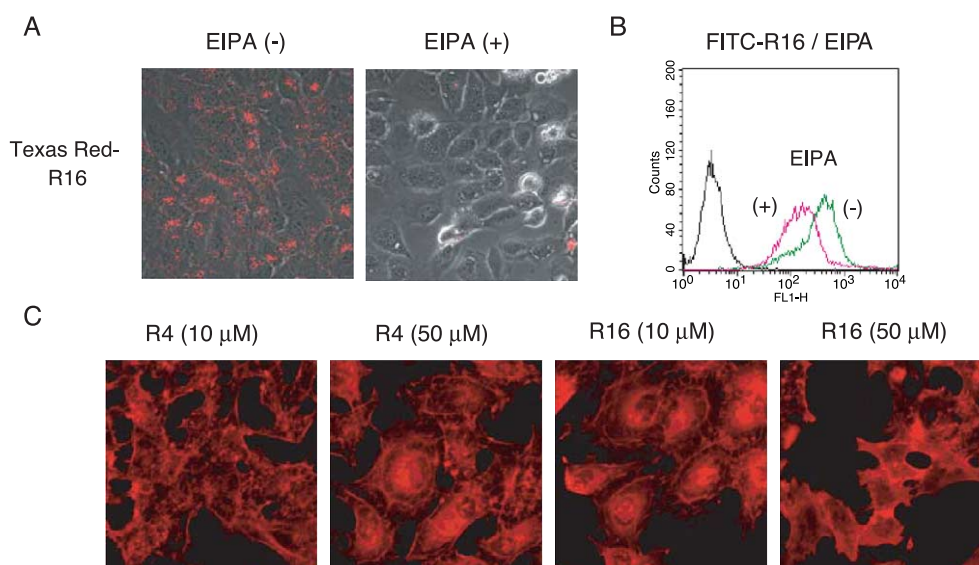


FIG. 4. Effects of chain length and macropinocytosis inhibitors on cellular uptake of oligoarginine peptides. The effect of EIPA (100 μ M) on the R16 peptide (10 μ M) uptake was examined by (A) confocal microscopy and (B) FACS analysis as described for Figs. 2A and 2B. Red line in (B), in the presence of EIPA; green line, in the absence of EIPA; black line, control cells. (C) Effects of 10 and 50 μ M R4 and R16 peptides on F-actin distribution. Conditions were the same as those described for Fig. 2E. (For interpretation of the references to colour in this figure legend, the reader is referred to the web version of this article.)

Incubation of cells with 10 μ M R4 peptide did not reveal any major actin rearrangement; however, we observed some effects when the concentration was raised to 50 μ M (Fig. 4C). It could therefore be reasoned that the lower internalization of the R4 peptide, compared to R8 and R16, is due to its inability to promote significant actin rearrangement and therefore macropinocytosis, as well as its presumably lower affinity to cell surfaces, although this requires further analysis.

Comparison of Penetratin and Oligoarginine Peptide Internalization

Penetratin is another representative carrier peptide [4,22] and intracellular delivery of a variety of molecules has been reported to be mediated by this peptide. Penetratin is originally derived from the third helix of the Antennapedia homeodomain protein (positions 43–58) and this peptide also contains seven basic amino acid residues in its sequence (RQIKIWFQNRRMKWKK). In contrast to Tat and oligoarginine peptides, penetratin contains hydrophobic amino acids such as tryptophan, and this property was suggested to be important for its internalization [4]. To estimate whether penetratin enters cells using a mechanism similar to that of the R8 peptide, we examined the effect of EIPA treatment on the internalization of penetratin.

Interestingly, in comparison to R8 and R16 peptides, there was no EIPA-dependent reduction in the cellular uptake of 10 μ M penetratin, as determined by confocal microscopy and FACS analysis (Figs. 5A and 5B). Treatment with penetratin (10 μ M) caused some F-actin

rearrangement, but the extent of rearrangement was considerably lower than that caused by R8 and R16 peptides (Fig. 5C). These results suggest a minor role for macropinocytosis in uptake of penetratin, in comparison with a greater dependence on this endocytic mechanism for uptake of R8 and R16 peptides. However, when cells were treated with 50 μ M penetratin, there was significant F-actin rearrangement and the cells resembled those incubated with 10 μ M R8 peptide (Fig. 5E). FACS analysis confirmed these observations and revealed a 43% decrease in penetratin uptake when the peptide concentrations were increased to 50 μ M (Fig. 5D).

Cytosolic Effects of an Apoptosis-Inducing Peptide Delivered by the Peptide Vectors

The peptides described are of fundamental importance as potential delivery vectors for proteins and other molecules from the endocytic pathway to the cytosol. In this study we use fluorescence microscopy and FACS analysis to measure the total amount of cell-associated peptides, including the fraction on the plasma membrane and that trapped in endosomes. Therefore it is not a true measurement of the amount of peptide that is released into the cytosol. We therefore utilized a functional assay to determine the fraction of internalized peptide that reaches the cytosol. For this we employed an apoptosis-inducing peptide (proapoptotic domain peptide, PAD) [23] as a measure of cellular activity induced by cytosolically located arginine peptide. PAD is an amphiphilic basic peptide comprising 14 residues of D-amino acids, D-(KLAKLAK)₂. The peptide has been

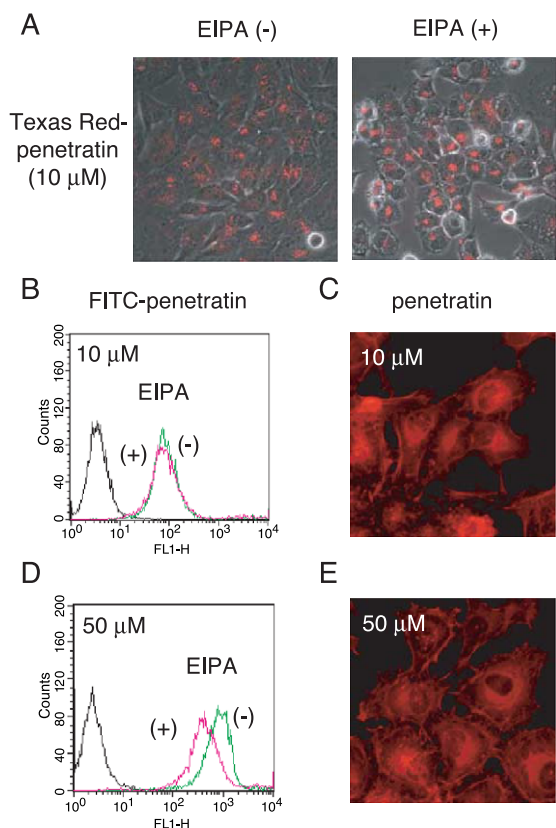


FIG. 5. Uptake of penetratin is not dependant on macropinocytosis. Cellular uptake of penetratin (10 μ M) in the presence and absence of EIPA by (A) confocal microscopy and (B) FACS analysis. Experimental conditions were the same as those described for Figs. 2A and 2B. (C) Effect of 10 μ M penetratin on F-actin distribution. The conditions were the same as those described for Fig. 2E. (D) FACS analysis of cellular uptake of penetratin (50 μ M) in the presence and absence of EIPA. (E) Effect of 50 μ M penetratin on F-actin distribution.

reported to cause mitochondrial membrane disruption and eventual apoptosis when internalized into cells, whereas, peripheral to the plasma membrane, the peptide was nontoxic. We connected arginine peptides (R4, R8, and R16) to the PAD peptide via disulfide cross-linking and assessed apoptotic cell death using the MTT assay [11] (Fig. 6A). We further confirmed induction of apoptosis by the PAD peptide intracellularly delivered by the R8 peptide by observing nucleosomal fragmentation of DNA (data not shown). Compared to untreated cells there was a general decrease in cell viability with increasing peptide length. The percentages of viable cells were 86, 72, and 56% for R4-, R8-, and R16-PAD treatment, respectively. We did not observe any significant toxicity of the PAD peptide (10 μ M) in the absence of arginine peptides. However, R16 peptide (10 μ M) showed some cytotoxicity (10%) to the cells, whereas that of R8 peptide was minimal (~1%) (Fig. 6A). The difference in the viability of the cells treated with R8-PAD and R16-PAD peptide was about 10%. Considering

the higher cytotoxicity of the R16 peptide itself, the amounts of cytosolic R16 and R8 peptides were comparable, or R16 was slightly higher under these conditions. Despite the fact that total cellular uptake of the R16 peptide is almost seven times higher than that of R8 peptide (Fig. 3B), a much larger fraction of R16 peptide may stick to membranes such as those of endosomes and consequently less would translocate into the cytosol. Observations supporting this hypothesis were recently reported by Zaro and Shen [24]. Via quantification of peptides in membrane-bound (presumably endosomal structures) and cytosolic fractions, they identified that the total cellular uptake of R15 peptide was almost five times greater than that of R9 peptide, but the amounts of each peptide in the cytosol were similar, indicating that the majority of the R15 peptides were trapped in endosomes.

We next examined the effects of EIPA on the cytosolic delivery of the PAD peptide by the peptide vectors. As EIPA is toxic to cells, the long incubation time employed with the above MTT assay leads to extensive cell death even in the absence of the PAD peptide. We therefore employed FACS analysis using fluorescein isothiocyanate (FITC)-conjugated annexin V [25] for assessing the effect of EIPA on the cytosolic delivery of the PAD peptide. Annexin V is a human anticoagulant that has high affinity for phosphatidylserine (PS). In normal healthy cells, PS is largely resident in the cytoplasmic leaflet of the plasma membrane, but in early apoptosis PS translocates to the extracellular leaflet and this can be evaluated with annexin V staining followed by FACS analysis. We treated HeLa cells with peptides in the absence and presence of EIPA (100 μ M) for 1 h as described in Fig. 2B and then conducted the annexin V assay as previously reported [25]. Since the disulfide cross-linked R8-PAD peptide used in Fig. 6A did not yield significant annexin V staining, presumably due to the possible partial cleavage of disulfide bonds in the process of internalization [26], we employed peptides in which the carrier vector and the PAD peptide were directly connected via two glycine residues. As vector peptides, we employed R8 (R8-GG-PAD), R16 (R16-GG-PAD), and penetratin (Pen-GG-PAD). In the absence of EIPA, the induction of annexin V staining was in the order R8-GG-PAD > R16-GG-PAD > Pen-GG-PAD (Fig. 6B). These results also suggested that the stronger binding of R16 peptide compared with that of R8 peptide to the endosomal membrane resulted in less efficient translocation into cytosol. Although we observed no significant effects of EIPA for Pen-GG-PAD-treated cells, treatment of the cells with R8-GG-PAD and R16-GG-PAD in the presence of EIPA (100 μ M) decreased annexin V staining. These results suggest that macropinocytosis contributes to the cytosolic release of R8-GG-PAD and R16-GG-PAD peptides, but not Pen-GG-PAD.

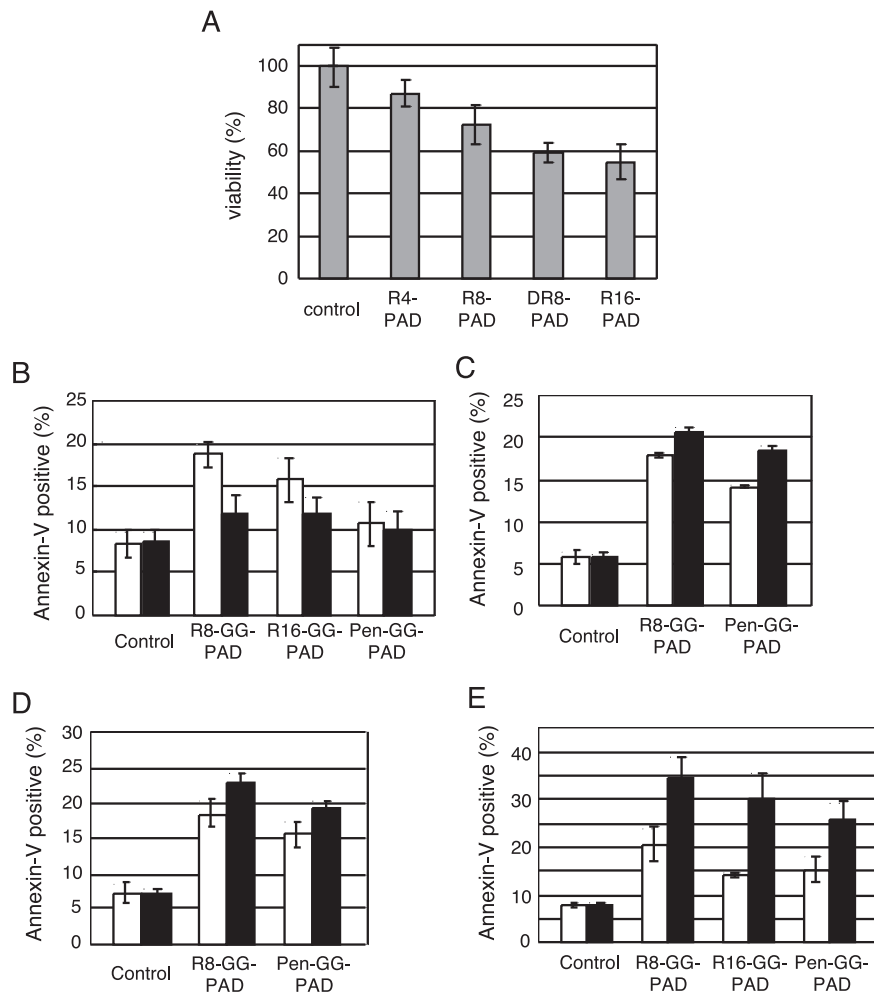


FIG. 6. Cytosolic activity of peptides conjugated to proapoptotic domain (PAD) peptide. (A) Apoptosis induced by PAD peptides enhanced by conjugation to R8 and R16. PAD peptide was conjugated to R4, R8, DR8, and R16 peptides via disulfide cross-linking. HeLa cells were treated with the peptide conjugates (10 μ M each) for 24 h; cell death was assessed by the MTT assay. Error bars represent the mean \pm standard error of three samples. Viability of the cells treated with the R4, R8, DR8, R16, and PAD peptides alone (10 μ M each) were 98 (\pm 1), 99 (\pm 1), 90 (\pm 2), 90 (\pm 3), and 101 (\pm 6)%, respectively. (B) Effects of EIPA (100 μ M) on apoptosis induction by the PAD peptides. The cells were treated with peptides in the absence and presence of EIPA (100 μ M) for 1 h as described for Fig. 2. Cytosolic activity of the peptides was assessed using annexin V assay as reported [25]. Open column, absence of EIPA; closed column, presence of EIPA. Error bars represent the mean \pm standard error of three samples. Effects of (C) wortmannin (400 nM) and (D) chloroquine (100 μ M) on apoptosis induction by the PAD peptides. Cells were treated with the above inhibitors in a serum-free medium for 30 min prior to treatment with the PAD peptides in a fresh serum-free medium in the presence of inhibitors for another 1 h, washed with PBS, and subjected to the annexin V assay. Open column, absence of inhibitors; closed column, presence of inhibitors. (E) Effects of low-temperature treatment on the internalization of the PAD peptides. Cells were pretreated at 4°C for 30 min prior to incubation with a medium containing the PAD peptides (10 μ M) at 4°C for 2 h. After the cells were washed with PBS, they were incubated in fresh medium in the absence of peptides at 37°C for 1 h, washed with PBS, and subjected to annexin V assay (closed column). Open columns represent the results of the cells treated with the peptides at 37°C for 2 h and then incubated at 37°C in the absence of peptides for another 1 h. Cells similarly treated with inhibitors in the absence of peptides were taken as controls.

We also examined the effects of wortmannin and chloroquine on peptide internalization and annexin V staining (Figs. 6C and 6D). Wortmannin, a phosphatidylinositol 3-kinase inhibitor, has multiple effects on endocytic processes [27], including inhibition of fluid-phase uptake and early endosome fusion [28,29], and chloroquine is a well-characterized inhibitor of endosomal acidification. We treated HeLa cells with R8-GG-

PAD and Pen-GG-PAD in the presence of wortmannin (400 nM, Fig. 6C) and chloroquine (100 μ M, Fig. 6D), respectively, for 1 h. In contrast to the results obtained from EIPA treatment, both wortmannin and chloroquine increased annexin V staining in cells incubated with 10 μ M R8-GG-PAD and Pen-GG-PAD conjugates. Wortmannin also increased the uptake of FITC-transferrin; however, we found that FITC-R8 uptake was inhibited by this

drug; penetratin uptake on the other hand is mediated via a wortmannin insensitive pathway (see Supplementary Material, Fig. S2).

To determine the dependency of endocytic processes on the effects of PAD peptides we conducted essentially the same experiments at 4°C. Surprisingly, we observed a dramatic increase in annexin V staining when the cells were treated with the PAD peptides at a low temperature (Fig. 6E). For these experiments, we treated the cells with the PAD peptides (10 μM) at 4°C for 2 h, followed by washout of the peptides and incubation of the cells in the absence of peptides at 37°C for another 1 h, thus allowing induction of apoptosis. Note that cellular uptake of vector peptides and the R8-PAD peptide was reduced by the same treatment (see Supplementary Material, Fig. S2). We further confirmed induction of apoptosis by microscopic observation of nuclear condensation 12 h after the peptide treatment. Again, treatment of cells with R8-PAD peptide at 4°C resulted in a higher extent of nuclear condensation compared with cells treated at 37°C (see Supplementary Material, Fig. S3). Since we observed no increase in annexin V staining for the control cells (i.e., in the absence of peptides), the observed induction in annexin V staining was not caused by the inhibitors and low-temperature treatment but rather by the PAD peptides themselves.

DISCUSSION

Recent data suggest that endocytic pathways are important for cellular uptake of the Tat peptide and Tat-fusion proteins. In this report, we demonstrate that a fraction of the endocytic uptake of oligoarginine peptide may be via macropinocytosis. In support of these observations, we also show that treatment of cells with oligoarginine peptides leads to rearrangement of the actin cytoskeleton. Induction of apoptosis resulting from oligoarginine-mediated cytosolic delivery of an apoptosis inducing peptide (PAD) was also suppressed by the macropinocytosis inhibitor, EIPA. Some reduction in R8 peptide uptake was also observed in nocodazole-treated cells, suggesting a role for microtubules in this process. By analyzing internalized R8 via live cell imaging, we observed dynamic fluorescent structures reminiscent of endocytic vesicles. The movement of these vesicles was inversely proportional to size, with the larger R8-positive structures being relatively nonmotile compared with their smaller counterparts. These may represent specific large vesicular compartments such as macropinosomes or endosomal swelling due to R8 complex formation. The degree of cellular uptake was also dependent on the physicochemical properties of carrier peptides. As was observed in the cellular uptake of oligoarginine peptides with different chain lengths, and other types of carrier peptides such as penetratin, subtle differences in the peptide sequence can have a significance influence on

their internalization characteristics. This has major implications for differential uses of these agents for therapeutic delivery of macromolecules such as genes and proteins into cells.

In this report, we demonstrate for the first time that the arginine peptides can induce cytoskeleton rearrangement, similar to that seen during macropinocytosis. Recently, a fusion protein of glutathione S-transferase and Tat protein caused stress fiber disassembly, peripheral retraction, and ruffle formation in human umbilical vein endothelial cells and human lung microvascular endothelial cells [30]. The arginine-rich basic domain of Tat as well as its cysteine-rich domain played a crucial role in the cytoskeletal rearrangement, which was induced via the activation of p21-activated kinase 1. Other studies describe sequence similarities between the basic domain of Tat and growth factors such as vascular endothelial growth factor (VEGF)-A and the activation of VEGF receptor 1 [31]. Although full-length Tat protein (86 residues) was employed for these experiments, the basic segment of Tat or oligoarginine peptides may have a similar ability to activate some plasma membrane receptors.

Several endocytic routes have been suggested for the cellular uptake of Tat and other arginine peptides [7,19–21,32]. Real-time imaging of R8 in cells shows highly dynamic R8-labeled structures, and numerous fusion and fission events are also observed. Although macropinocytosis is shown to be one of the major pathways of internalization of oligoarginine peptides, it seems possible that cellular uptake occurs via more than one pathway depending on, for example, the properties of carrier peptides and cargoes, peptide concentrations, and the choice of selected cell lines. Differential sorting to alternative endocytic structures after uptake could also be possible. These all suggest that interpretation of data is extremely complex and open to a number of different interpretations. Examining the cellular uptake of a fusion protein of Tat (48–58) and EGFP, Fittipaldi and colleagues concluded that caveolae-mediated endocytosis was the major internalization pathway of the fusion protein [21]. Their fusion protein showed little colocalization with transferrin; however, the cellular uptake was not affected by nocodazole. Also, the speed of internalization of the fusion protein seemed much slower than that of the oligoarginine peptides compared with our previous observations [12]—almost 10 h was necessary to obtain maximum cellular uptake for the fusion protein, whereas less than 1 h was necessary for the Tat (48–60) peptide. They also reported that the vesicles containing the fusion protein did not show apparent movement over a 40-s period. Another recent report suggested that the sizes of delivered molecules could have a major impact on their method of internalization and further endocytic delivery [33]. Presumably, both the peptides and their cargoes will affect internalization and cytosol release. This, however, needs to be determined if these

systems are to be effectively utilized as drug delivery vehicles.

Wortmannin is a powerful inhibitor of macropinocytosis [34] and we show inhibition of R8 uptake in the presence of this drug and, in agreement with this, with EIPA (Fig. S2A in Supplementary Material). We therefore conclude that macropinocytosis also plays a crucial role in the cellular uptake of oligoarginine peptides. As expected, transferrin accumulation was increased in wortmannin-treated cells, most probably due to the strong inhibition of transferrin recycling by this drug [35,36]. Wortmannin also inhibits fluid-phase uptake [28] and we cannot refute the fact that a portion of the wortmannin-induced inhibition was due to a reduction in fluid phase uptake. Penetratin uptake is, however, unaffected by wortmannin or EIPA, suggesting a distinct pathway for its uptake compared with the arginine peptides used in this study.

Data from this and other studies show that endocytosis is a major contributor to internalization of these peptides, and we also show using functional assays that a fraction of the cargo is translocated into the cytosol. Whether this is due to effects of these peptides on endosome integrity, membrane potential, orientation of lipids, or combinations of these still awaits clarification [37–39]; endosome disruption enhances the functional cytosolic delivery of Tat-fusion proteins. This juncture is one of the most critical stages for peptide-mediated delivery to cells, and further study is necessary to clarify the translocation mechanism from the endosome.

Despite the obvious contribution of endocytosis to peptide uptake we still observe significant cell-associated R8 peptide when incubations are performed at 4°C; cellular distribution of the peptide is also different from that internalized at 37°C. Using confocal sections we did, however, observe that the majority of label was confined to specific areas of the cell close to or on the plasma membrane. It may therefore be that the mechanism of peptide integration with cellular membranes at 4°C is different from that in cells kept at 37°C. We were, however, surprised to observe that a higher cytosolic activity was attained in cells treated with the PAD peptide using a low-temperature treatment compared with one at 37°C. It may be possible that, under conditions under which classical endocytic pathways are inhibited, the peptide that is integrated with the plasma membrane is then more efficiently translocated to the cytosol. We cannot, however, currently conclude whether this temperature effect is a unique feature of the PAD conjugates. More information is therefore required to elucidate this phenomenon and whether this is also observed for the combination of other vectors or cargoes.

In conclusion this study highlights that subtle differences in the structures of carrier peptides have a significant influence in the methods of internalization and that, depending on the conditions of administra-

tion, alternative pathways can be employed when others are inhibited. As these peptides are likely to have unique cell binding characteristics and specific mechanisms of interaction with the plasma membrane, it is unlikely that one mechanism will explain their endocytosis profiles. Further work is therefore required to understand better the interaction of the peptides with the cell surface, the structural requirements that mediate the mechanism of uptake into distinct classes of endosomes, and the processes by which the peptides translocate into the cytosol. These studies are currently under way in our laboratories.

MATERIALS AND METHODS

Cell culture. Human cervical cancer-derived HeLa cells were maintained in α -minimum essential medium (α -MEM) with 10% heat-inactivated calf serum. Cells were grown on 60-mm dishes and incubated at 37°C under 5% CO₂ to approximately 70% confluence. A subculture was performed every 3–4 days.

Peptide internalization and microscopic observation. For each assay, 2×10^5 cells were plated into 35-mm glass-bottomed dishes (Iwaki) and cultured for 48 h. After complete adhesion, the culture medium was exchanged. The cells were then incubated at 37°C with fresh medium (200 μ l) containing the peptides. Cells were washed five times with cold PBS. Distribution of the fluorescently labeled peptides was analyzed using a confocal scanning laser microscope LSM 510 (Zeiss) equipped with a 40 \times objective in 4°C medium *without fixing the cells*. For examination of the effect of various inhibitors or effectors on the cellular uptake of the peptides, the cells were pretreated with these reagents as described in the figure legends and then treated with peptides in the continued presence of the reagents. After washing with PBS, the cells were subjected to the microscopic observation. Unless otherwise mentioned, cells were incubated at 37°C in an atmosphere of 5% CO₂.

Cell ruffling assay. HeLa cells were seeded into eight-well Lab-Tek-II chamber slides (Nalge Nunc) at a density of 2.4×10^4 cells per well in α -MEM containing 10% heat-inactivated calf serum for 48 h. The medium was replaced by fresh medium containing 1% BSA instead of 10% calf serum, and cells were incubated for 24 h. After being washed with medium, the cells were treated with peptides (without fluorescent moieties) (10 μ M) or EGF (10 nM) in α -MEM for 30 min. The cells were washed three times with PBS, fixed with 4% paraformaldehyde at room temperature for 10 min, treated with 0.5% Triton X-100 in PBS at room temperature for 2 min, and then washed with PBS again. Cellular F-actin was stained with phalloidin-TRITC as described [40] and observed using an IX-70 Olympus fluorescence microscope equipped with a 20 \times objective.

Flow cytometry. To analyze the internalization of the peptides by FACS, 1.5×10^5 HeLa cells in fresh culture medium (1.5 ml) were plated into 12-well microplates (Iwaki) and cultured for 48 h in α -MEM containing 10% heat-inactivated calf serum. After complete adhesion the cells were incubated at 37°C for 1 h with fresh medium (400 μ l) containing peptides prior to washing with PBS. The cells were then treated with 0.01% trypsin (400 μ l) at 37°C for 10 min prior to addition of 600 μ l of PBS. The cells were centrifuged at 2000 rpm (400g) for 5 min and after the supernatant was removed, they were washed with 1 ml of PBS and centrifuged at 2000 rpm for 5 min. After this washing cycle was repeated, the cells were suspended in PBS (1 ml) and subjected to fluorescence analysis on a FACScalibur (BD Biosciences) flow cytometer using 488-nm laser excitation and a 515- to 545-nm emission filter.

MTT assay. The MTT assay was conducted essentially as previously described [11]. Briefly, cells (1.5×10^3 /well) were cultured in 96-well microtiter plates in α -MEM with 10% heat-inactivated calf serum in the

presence of peptide conjugates. The cells were incubated with the peptide conjugates (total volume, 50 μ l) at 37°C under 5% CO₂ for 24 h. MTT in PBS (0.05 mg/10 μ l) was added to the above medium, and the cells were further incubated for 4 h. The precipitated MTT formazan was dissolved overnight in 0.04 N HCl in isopropanol (100 μ l). The absorbance at 570 nm was then measured. Cell viability was expressed as the A570 ratio of peptide-treated cells compared with cells incubated in the absence of peptide.

Annexin V assay. Cells were stained with FITC-annexin V according to the manufacturer's specification using Vybrant Apoptosis Assay Kit No. 3 (Molecular Probes). For analysis, 1.0×10^5 cells were plated on a 24-well plate and incubated for 48 h. Cells were treated with the PAD peptides as described in the legend for Fig. 6, harvested by trypsinization, and then washed with PBS. Cells were suspended in annexin V binding buffer (10 mM Hepes, 140 mM NaCl, and 2.5 mM CaCl₂, pH 7.4) (100 μ l) and then incubated with FITC-annexin V (5 μ l) and the PI working solution (100 μ g/ml, 1 μ l) at room temperature for 15 min. After the incubation period, the cells were diluted with annexin V binding buffer (800 μ l). Apoptotic cells, which were positive for FITC-annexin V and negative for PI staining, were analyzed by FACS.

Description of materials and peptide synthesis is shown in the Supplementary Material.

APPENDIX A. SUPPLEMENTARY DATA

Supplementary data associated with this article can be found, in the online version, at doi:10.1016/j.ymthe.2004.08.010.

RECEIVED FOR PUBLICATION FEBRUARY 27, 2004; ACCEPTED AUGUST 19, 2004.

REFERENCES

- Futaki, S., Goto, S., and Sugiura, Y. (2003). Membrane permeability commonly shared among arginine-rich peptides. *J. Mol. Recognit.* **16**: 260–264.
- Wadia, J. S., and Dowdy, S. F. (2003). Modulation of cellular function by TAT mediated transduction of full length proteins. *Curr. Protein Pept. Sci.* **4**: 97–104.
- Wright, L. R., Rothbard, J. B., and Wender, P. A. (2003). Guanidinium rich peptide transporters and drug delivery. *Curr. Protein Pept. Sci.* **4**: 105–124.
- Prochiantz, A. (2000). Messenger proteins: homeoproteins, TAT and others. *Curr. Opin. Cell Biol.* **12**: 400–406.
- Langel, Ü. (2002). *Cell-Penetrating Peptides: Processes and Applications*. CRC Press, Boca Raton, FL.
- Vivès, E., Brodin, P., and Lebleu, B. (1997). A truncated HIV-1 Tat protein basic domain rapidly translocates through the plasma membrane and accumulates in the cell nucleus. *J. Biol. Chem.* **272**: 16010–16017.
- Richard, J. P., et al. (2003). Cell-penetrating peptides: a reevaluation of the mechanism of cellular uptake. *J. Biol. Chem.* **278**: 585–590.
- Wender, P. A., Mitchell, D. J., Pattabiraman, K., Pelkey, E. T., Steinman, L., and Rothbard, J. B. (2000). The design, synthesis, and evaluation of molecules that enable or enhance cellular uptake: peptidic molecular transporters. *Proc. Natl. Acad. Sci. USA* **97**: 13003–13008.
- Umezawa, N., Gelman, M. A., Haigis, M. C., Raines, R. T., and Gellman, S. H. (2002). Translocation of a beta-peptide across cell membranes. *J. Am. Chem. Soc.* **124**: 368–369.
- Rueping, M., Mahajan, Y., Sauer, M., and Seebach, D. (2002). Cellular uptake studies with beta-peptides. *ChemBioChem* **3**: 257–259.
- Futaki, S., et al. (2001). Arginine-rich peptides: an abundant source of membrane-permeable peptides having potential as carriers for intracellular protein delivery. *J. Biol. Chem.* **276**: 5836–5840.
- Suzuki, T., Futaki, S., Niwa, M., Tanaka, S., Ueda, K., and Sugiura, Y. (2002). Possible existence of common internalization mechanisms among arginine-rich peptides. *J. Biol. Chem.* **277**: 2437–2443.
- Futaki, S., Nakase, I., Suzuki, T., Zhang, Y., and Sugiura, Y. (2002). Translocation of branched-chain arginine peptides through cell membranes: flexibility in the spatial disposition of positive charges in membrane-permeable peptides. *Biochemistry* **41**: 7925–7930.
- Conner, S. D., and Schmid, S. L. (2003). Regulated portals of entry into the cell. *Nature* **422**: 37–44.
- Swanson, J. A., and Watts, C. (1995). Macropinocytosis. *Trends Cell Biol.* **5**: 424–428.
- Meier, O., et al. (2002). Adenovirus triggers macropinocytosis and endosomal leakage together with its clathrin-mediated uptake. *J. Cell Biol.* **158**: 1119–1131.
- Torchilin, V. P., Rammohan, R., Weissig, V., and Levchenko, T. S. (2001). TAT peptide on the surface of liposomes affords their efficient intracellular delivery even at low temperature and in the presence of metabolic inhibitors. *Proc. Natl. Acad. Sci. USA* **98**: 8786–8791.
- Wadia, J. S., Stan, R. V., and Dowdy, S. F. (2004). Transducible TAT-HA fusogenic peptide enhances escape of TAT-fusion proteins after lipid raft macropinocytosis. *Nat. Med.* **10**: 310–315.
- Potocky, T. B., Menon, A. K., and Gellman, S. H. (2003). Cytoplasmic and nuclear delivery of a TAT-derived peptide and a beta-peptide after endocytic uptake into HeLa cells. *J. Biol. Chem.* **278**: 50188–50194.
- Thorén, P. E., Persson, D., Isakson, P., Gokso, M., Onfelt, A., and Norden, B. (2003). Uptake of analogs of penetratin, Tat (48–60) and oligoarginine in live cells. *Biochem. Biophys. Res. Commun.* **307**: 100–107.
- Fittipaldi, A., et al. (2003). Cell membrane lipid rafts mediate caveolar endocytosis of HIV-1 Tat fusion proteins. *J. Biol. Chem.* **278**: 34141–34149.
- Derosi, D., Joliot, A. H., Chassaing, G., and Prochiantz, A. (1994). The third helix of the Antennapedia homeodomain translocates through biological membranes. *J. Biol. Chem.* **269**: 10444–10450.
- Ellerby, H. M., et al. (1999). Anti-cancer activity of targeted pro-apoptotic peptides. *Nat. Med.* **5**: 1032–1038.
- Zaro, J. L., and Shen, W. (2003). Quantitative comparison of membrane transduction and endocytosis of oligopeptides. *Biochem. Biophys. Res. Commun.* **307**: 241–247.
- Futaki, S., et al. (2004). Arginine carrier peptide bearing Ni(II) chelator to promote cellular uptake of histidine-tagged proteins. *Bioconjugate Chem.* **15**: 475–481.
- Feener, E. P., Shen, W. C., and Ryser, H. J. (1990). Cleavage of disulfide bonds in endocytosed macromolecules: a processing not associated with lysosomes or endosomes. *J. Biol. Chem.* **265**: 18780–18785.
- Backer, J. M. (2000). Phosphoinositide 3-kinases and the regulation of vesicular trafficking. *Mol. Cell. Biol. Res. Commun.* **3**: 193–204.
- Clague, M. J., Thorpe, C., and Jones, A. T. (1995). Phosphatidylinositol 3-kinase regulation of fluid phase endocytosis. *FEBS Lett.* **367**: 272–274.
- Jones, A. T., and Clague, M. J. (1995). Phosphatidylinositol 3-kinase activity is required for early endosome fusion. *Biochem. J.* **311**: 31–34.
- Wu, R. F., Gu, Y., Xu, Y. C., Mitola, S., Bussolino, F., and Terada, L. S. (2004). Human immunodeficiency virus type 1 Tat regulates endothelial cell actin cytoskeletal dynamics through PAK1 activation and oxidant production. *J. Virol.* **78**: 779–789.
- Mitola, S., et al. (1997). Tat-human immunodeficiency virus-1 induces human monocyte chemotaxis by activation of vascular endothelial growth factor receptor-1. *Blood* **90**: 1365–1372.
- Fischer, R., Kohler, K., Fotin-Mleczek, M., and Brock, R. (2004). A stepwise dissection of the intracellular fate of cationic cell-penetrating peptides. *J. Biol. Chem.* **279**: 12625–12635.
- Rejman, J., Oberle, V., Zuhorn, I. S., and Hoekstra, D. (2004). Size-dependent internalization of particles via the pathways of clathrin- and caveolae-mediated endocytosis. *Biochem. J.* **377**: 159–169.
- Araki, N., Johnson, M. T., and Swanson, J. A. (1996). A role for phosphoinositide 3-kinase in the completion of macropinocytosis and phagocytosis by macrophages. *J. Cell Biol.* **135**: 1249–1260.
- Spiro, D. J., Boll, W., Kirchhausen, T., and Wessling-Resnick, M. (1996). Wortmannin alters the transferrin receptor endocytic pathway in vivo and in vitro. *Mol. Biol. Cell* **7**: 355–367.
- Shpetner, H., Joly, M., Hartley, D., and Corvera, S. (1996). Potential sites of PI-3 kinase function in the endocytic pathway revealed by the PI-3 kinase inhibitor, wortmannin. *J. Cell Biol.* **132**: 595–605.
- Terrone, D., Sang, S. L., Roudaia, L., and Silviu, J. R. (2003). Penetratin and related cell-penetrating cationic peptides can translocate across lipid bilayers in the presence of a transbilayer potential. *Biochemistry* **42**: 13787–13799.
- Del Gaizo Moore, V., and Payne, R. M. (2004). Transactivator of transcription fusion protein transduction causes membrane inversion. *J. Biol. Chem.* **279**: 32541–32544.
- Caron, N. J., Quenneville, S. P., and Tremblay, J. P. (2004). Endosome disruption enhances the functional nuclear delivery of Tat-fusion proteins. *Biochem. Biophys. Res. Commun.* **319**: 12–20.
- Wulf, E., Deboben, A., Bautz, F. A., Faulstich, H., and Wieland, T. (1979). Fluorescent phalloxin, a tool for the visualization of cellular actin. *Proc. Natl. Acad. Sci. USA* **76**: 4498–4502.